Published in final edited form as:
J Biomed Mater Res B Appl Biomater. 2004 July 15; 70(1): 56–65. doi:10.1002/jbm.b.30012.

Micromechanical Analysis of Dentin/Adhesive Interface by the Finite Element Method

Anil Misra[1], **Paulette Spencer**[2], **Orestes Marangos**[1], **Yong Wang**[2], and **J. Lawrence Katz**[1,2]
[1]School of Computing and Engineering, University of Missouri—Kansas City, Kansas City, MO
[2]Department of Oral Biology, University of Missouri—Kansas City, Kansas City, MO

Abstract

The interfacial microstructure and spatial distribution of the modulus of elasticity have a profound effect on load transfer at the dentin/adhesive (d/a) interface. The microstructure is influenced by the varying degree of demineralization of intertubular and peritubular dentin during etching as well as the depth of adhesive penetration into the hybrid layer. These factors lead not only to a unique microstructure in the vicinity of the dentinal tubules, but also to a mechanically graded hybrid layer. This article investigates the micromechanical stress distribution at a d/a interface with the use of finite element analysis (FEA). Such analysis is now feasible given the newly measured moduli of elasticity at micro- and nanoscales. The results indicate that the morphological and micromechanical properties of the d/a interface affects the stress field such that the fracture/failure is likely to initiate in the stress-concentration zone of peritubular dentin next to the hybrid/exposed-collagen layer. The results suggest that devising a full-depth high modulus hybrid layer may considerably reduce the stress concentration zone and the magnitude of stress concentration in the peritubular dentin next to the hybrid/exposed-collagen layer.

Keywords

finite element; dentin/adhesive; collagen; micromechanics; interface

INTRODUCTION

Replacement of failed restorations accounts for nearly 75% of operative dentistry,[1,2] and this emphasis on replacement therapy is expected to grow as the public's concern about mercury release from dental amalgam forces dentists to select alternative restorative materials, for example, composite resin. The failure rate for large to moderate posterior composite restorations can be 2–3 times that of high copper amalgam.[3] The higher failure rate means increased frequency of replacement with loss of additional tooth structure; that is, sound tooth structure is inevitably removed with each replacement.[4,5] Results from previous clinical studies have suggested that the durability of composite restorations, particularly Class II composites, depends on the quality of the bond formed at the dentin/adhesive interface (d/a).

Current adhesives attach to dentin via a hybrid layer (HL).[6,7] The ideal HL is formed when adhesive resin penetrates the demineralized dentin, infiltrating the exposed collagen to create a continuous integrated collagen/resin biopolymer that bonds the bulk adhesive to the

Correspondence to: Anil Misra, 350H Flarsheim Hall, 5100 Rockhill Road, University of Missouri—Kansas City, Kansas City, MO 64110 (misraa@umkc.edu.

intact dentin.[8–10] Demineralized dentin is 30% collagen and 70% water; adhesive must diffuse through water to form a HL.[7] Use of micro-Raman spectroscopy (μRS) and scanning acoustic microscopy (SAM) led to the determination, for the first time, of the *in situ* molecular composition and micromechanical properties of the HL.[11–15] The results indicated a serious limitation of BisGMA/HEMA adhesive–physical separation upon mixing with water in the demineralized dentin, leading to partitioning of the adhesive into hydrophobic BisGMA-and hydrophilic HEMA-rich phases.[16] The critical dimethacrylate (BisGMA), the component contributing most to the cross-linked polymeric adhesive, infiltrated only a fraction of the wet, demineralized intertubular dentin. Nearly half of the interface was predominantly collagen, with contribution from the hydrolytically unstable monomethacrylate HEMA.

Because of the nondestructive, noninvasive nature of the μRS technique, it was possible to analyze the same specimens described above with the use of SAM.[13]]. SAM was used in the burst mode to study the micromechanical properties of the d/a interface. The elastic moduli of the components of the interface were determined by comparing the recorded acoustic impedance values to a set of calibration curves generated on standard materials. The elastic modulus for dentin ranged from 13 GPa (partially demineralized) to 28 GPa; adhesive 5 GPa; and for unprotected collagen at the interface, <2 GPa. These data were correlated with the μRS results and based on this correlation, the lowest value correlates with the region of the interface that was spectroscopically dominated by features associated with Type I collagen from the demineralized dentin matrix. As described in recent publications,[13–15,17] by combining the unique capabilities of μRS, SAM, and optical microscopy, chemical, mechanical, and morphologic characterization over the same small region of the d/a interface can be performed. The combination of μRS and SAM allowed the determination of the molecular structure and elastic properties of the d/a interface *in situ*; because both of these techniques are nondestructive, the measurements were completed on the same small region of the interface of the same specimen. Figure 1 shows examples of images of the same small region, obtained from μRS, SAM, and an optical microscope.

Based upon the chemical, micromechanical, and morphologic characterization derived from the use of μRS, SAM, and optical microscopy, the dentin/adhesive interface may be idealized as depicted in Figure 2. In this idealization, the dentin/adhesive interface is considered to be composed of the dental composite, the hybrid layer, the demineralized dentin collagen, and the adhesive. It is well known that the adhesive penetrates the tubule orifice, forming adhesive tags that form imperfect bonds with the lumen walls. Furthermore, the adhesive infiltrates the demineralized dentin forming the hybrid layer. There are two phenomena that are noteworthy with respect to the formation of the hybrid layer:

1. The demineralization due to etching is considerably more in the intertubular dentin as opposed to peritubular dentin, such that the adhesive infiltration in the demineralized intertubular dentin is at greater depths as seen from the dentin/adhesive interface analysis with the use of μRS (see Figure 1 and discussion in Spencer et al.[11]).
2. The adhesive infiltration into the demineralized dentin diminishes with depth, such that the adhesive– collagen hybrid layer is graded with depth.[11–17]

These phenomena result in a unique structure in the vicinity of the tubules and a mechanically graded hybrid layer. Moreover, in the cases where the adhesive infiltration is not to the full depth of the demineralized intertubular dentin, an exposed-collagen layer may exist below the hybrid layer, as observed by Katz et al.[13] through SAM measurements. SAM measurements have also shown that the intertubular dentin below the exposed-collagen (or fully demineralized) zone may also experience partial demineralization, such that in the

vicinity of the interface, the intertubular dentin may also be considered to be mechanically graded.

Table I compiles the elastic and geometrical properties of the interface components based upon published values. Kinney et al.[18] have measured the elasticity modulus of peritubular dentin to have a mean value of 28.6 GPa, and that of intertubular dentin to have a mean value of 20 GPa. As mentioned previously, more recent measurements by Katz et al.,[13] have shown that in the vicinity of the interface, the intertubular dentin may have elasticity modulus as low as 13 GPa because of partial demineralization. Thus, the intertubular dentin below the hybrid/exposed-collagen layer is expected to have a modulus gradient from 13 GPa ramping up to 20 GPa. Similarly, based upon limited mechanical properties measured by Katz et al.[13] and morphological arguments, the hybrid/exposed-collagen layer is expected to have a modulus gradient from a modulus of 5 GPa close to the adhesive layer down to the exposed-collagen modulus of ≈1 GPa. The thicknesses of various components have large variations depending upon the dentin location, preparation method, and the adhesive and composite utilized.

In bonded joints such as the d/a interface, fractures generally initiate at sites where stress tends to concentrate (e.g. flaws, defects, or voids). With the use of finite element analyses, previous authors have demonstrated that it is very likely that defects dominate the propagation of fracture at d/a interfaces.[19,20] Adhesive phase separation could simulate a defect or stress concentrator. Potentially, stress would concentrate at the boundary between the relatively stiff BisGMA-rich phase and the very weak HEMA-rich phase. Bond failure in an otherwise ideal adhesive joint would initiate at these sites of local stress concentrations. The structure of the dentin/adhesive interface, as well as the modulus of elasticity of the dental composite, the hybrid layer, the demineralized dentin collagen, and the adhesive, profoundly affects the load transfer at the dentin/adhesive interface. This article examines the hypothesis that the moduli of elasticity at the interface will lead to stress concentrations that will result in failure initiation at the interface. The *in situ* microstructural and micromechanical property measurements obtained from μRS, SAM, and optical microscopy are used in FE analyses to predict stress concentrations and distributions at the interface under tensile loading.

MATERIALS AND METHODS

For the purposes of a two-dimensional FE analysis of stress distribution at the dentin/adhesive interface, a conceptual thin sample of restored tooth subjected to tensile loading is considered, as depicted in Figure 3. Plane stress or axisymmetric elements may be used in the analysis to mimic the tension test, depending upon the orientation of the thin sample. Thin samples from two potential orientations may be considered as shown in the tooth cross section in Figure 3: (a) along the circumferential plane, and (b) along the radial plane. The sample extracted from the circumferential plane may be reasonably modeled with plane stress condition, such that out-of-the-plane stresses are zero, whereas the sample extracted from the radial plane is expected to experience axisymmetric loading conditions. For the circumferential sample, plane stress elements are considered appropriate in all d/a interface components, including the peritubular dentin, as out-of-plane stress may be shown to have a minimal influence on the stress distributions. For the radial sample, axisymmetric elements maybe used for all d/a interface components. FE analyses were performed for both plane stress and axisymmetric conditions; however, this article reports the results obtained from the analysis under plane stress conditions. It is noted that qualitatively identical results were obtained for analysis under axisymmetric conditions. The stress distributions within the dentin/adhesive interface were computed based upon the schematic interface structure shown in Figure 2. For computational efficiency, a computational unit cell, which is

representative of the interface, was identified as depicted in Figure 1. Elastic stress analysis of the two-dimensional unit cell subjected to a tensile load in the direction of the tubules was performed with a widely used commercial finite element (FE) package—I-DEAS. The finite element components and discretization mesh for this analysis are also shown in Figure 3.

Based upon the geometrical properties of the interface components, the computational unit-cell sizes are selected to be 14.0 –22.0 μm high and 5.2–9.0 μm wide, depending upon the width of the peritubular and intertubular dentin. For accuracy of calculations, element size is chosen to be 0.1 μm. The dental composite represented by yellow zone is taken to be 6.0 μm thick, and the adhesive and adhesive tags represented by the red zone are 2.0 and 1.0 μm thick, respectively. The intertubular dentin is divided into two 2.0-μm-thick zones of elastic modulus 13 and 20 GPa, respectively. The width of the peritubular dentin represented by dark green zone is varied from 0.6 –1.0 μm, whereas that of the intertubular region is varied from 2.0 to 5.0 μm. Furthermore, the thickness of the hybrid/exposed-collagen layer is varied from 2.0 to 10.0 μm. The elastic moduli of the hybrid/exposed-collagen layer are taken to be graded from 4 GPa close to the adhesive layer to 1 GPa in the exposed collagen at the bottom of the hybrid layer. The gradation in the elastic moduli of the hybrid/exposed-collagen layer is represented in the FE model by considering this layer to be composed of several sublayers of equal thickness and varying the elastic moduli of the sublayers from 4 GPa to 1 GPa. Perfect bonding is assumed among the various d/a interface components, except for that between the adhesive tags and the tubule walls. The imperfect bonding between the adhesive tags and the tubule walls is represented by a thin layer of extremely low modulus material.

For the circumferential sample (plane stress condition), the periodicity of the computational cell in the horizontal direction is considered by applying periodic boundary conditions on the nodes along the boundaries in the horizontal direction, given by:

$$u(0,y)=-u(B,y) \quad \text{and} \quad v(0,y)=v(B,y) \quad (1)$$

where u and v are the nodal displacements along x and y directions, respectively, and B is the width of the unit cell. For the radial sample (axisymmetric condition), the horizontal boundaries are restrained as follows:

$$u(0,y)=0 \quad \text{and} \quad v(0,y)=v(B,y) \quad (2)$$

The bottom boundary nodes of the peritubular and intertubular dentin are restrained in the vertical directions. The bottom boundary nodes of the adhesives tags are unconstrained, as these are not attached at their base. A tensile force equivalent to 20 MPa is applied on the top boundary nodes of the dental composite. This applied stress is chosen to investigate the stress distributions close to the tensile strength of dentin/adhesive interfaces. Phrukkanon, Burrow, and Tyas[21] have reported that the dentin/adhesive interface tensile strength ranges from 15 to 30 MPa, depending upon dentin position.

RESULTS

Effect of Adhesive Infiltration on Stress Distribution

As discussed earlier, adhesive may not completely or, in some cases, effectively infiltrate into the demineralized dentin. The effect of adhesive infiltration upon stress distribution may be illustrated by considering the following two infiltration profiles:

1. Linear profile: hybrid layer is linearly graded with underlying exposed collagen because of partial adhesive infiltration

2. Full infiltration: hybrid layer is uniform and extends to the partially demineralized dentin as a result of full adhesive infiltration.

For the case of linear profile, the elastic moduli of the hybrid/exposed-collagen layers are linearly graded from 4 GPa at the top to 1 GPa at the bottom. For the case of full infiltration, the hybrid layer is considered to be homogeneous with elastic modulus of 4 GPa. Figure 4(a, b) give the major principal stress distribution and the Von Mises stress distribution in the unit cell for both linear profile and full infiltration. Although the major principal stress is a good index for identifying fractures that may initiate at small defects, the Von Mises stress may be useful in identifying plastic yielding within the material. Because the failure mechanisms that occur at the microscales within the d/a interface are as yet unclear, the FE analysis results are presented in terms of both the major principal stress and the Von Mises stress. From the stress distributions in Figure 4(a, b), it can be seen that the stresses concentrate in two zones: Zone 1—the peritubular dentin in the proximity of the hybrid layer, and Zone 2—at the adhesive/peritubular dentin interface. The stress concentration in Zone 1 is caused by the presence of the stiff peritubular dentin in proximity of a relatively soft hybrid layer. In contrast, the stress concentration in Zone 2 is a consequence of the assumption that there is a perfect bond between the adhesive layer and top of the peritubular dentin.

The major principal stress distribution for the linear-profile case shows that tensile stresses in the peritubular dentin near the hybrid layer (Zone 1) could be as high as 78 MPa, which is 3.9 times the applied tensile stress of 20 MPa. If this tensile stress is compared to the measured tensile strengths of dentin based upon uniaxial tension tests,[22] it can be seen that this stress greatly exceeds the demineralized human dentin tensile strength, which has been reported to range from 24.5 to 39.5 MPa, and approaches the mineralized dentin tensile strength, which has been reported to vary from 90 to 130 MPa. Furthermore, the Von Mises stress, which is obtained as the square root of the second invariant of the deviatoric stress tensor and is proportional to the shearing stress on the octahedral plane, also concentrates in the same location within the peritubular dentin and has a magnitude as high as 3.80 times the applied stress. In contrast, the maximum stresses are up to 10% smaller for the full-infiltration case as compared to the linear-profile case, even though the stress concentrations occur in similar locations. It can also be observed that the stress concentration zones are visibly smaller for the full-infiltration case as compared to the linear-profile case. The contrast between the two cases is more notable for the major principal stress distributions in the peritubular zone next to the hybrid layer (Zone 1). As can be seen from Figure 4(a) for the full-infiltration case, the major principal stress concentration zone in this region is considerably smaller. Moreover, for the full-infiltration case, the maximum major principal stress in this zone is in the range of 54–63 MPa, which is 2.70–3.15 times the applied stress. In contrast, for the linear-profile case, the maximum major principal stress in the same zone is 2.70–3.90 times the applied stress. Similar stress conditions are seen from the Von Mises stress distributions in Figure 4(b). Thus, for the full-infiltration case, wherein the hybrid layer has full adhesive penetration, the likelihood of failure initiating in this peritubular region is much less than that for the linear-profile case, wherein the adhesive penetration is partial, such that there is a presence of exposed-collagen layer.

The effect of adhesive infiltration is further investigated by examining the stress distributions for four different adhesive infiltration profiles such that the hybrid/exposed-collagen layer elastic moduli is given by Figure 5. The full-infiltration and Profile 2 curves represent the cases in which the adhesive infiltration through the hybrid layer is successful, whereas the linear-profile and Profile 3 curves represent the cases in which adhesive infiltration is partial. In these calculations, the thickness of the hybrid/exposed-collagen layer is taken to be 10 μm. Table II tabulates the maximum Von Mises and major principal

stresses at the two stress concentration zones within the d/a interface for the four adhesive infiltration profiles. As expected, the maximum stresses are the lowest for the full-infiltration profile and are the highest for Profile 3. It is also noted that the stress concentration will be further exacerbated for cases with lower elastic moduli or nonlinear gradation of elastic moduli in the hybrid/exposed-collagen layers that could result from a poor adhesive penetration or adhesive phase separations.

Effect of Hybrid/Exposed-Collagen Layer Thickness on Stress Distribution

Next the effect of varying hybrid/exposed-collagen layer thickness upon stress concentration is examined. In these computations, a linear profile is assumed for adhesive infiltration and the hybrid/exposed-collagen layer thickness is taken to vary from 2 to 10 μm. Figure 6(a, b) gives the variation of stress concentration factors, defined as the ratio of maximum stress and applied stress at the two stress concentration zones, with hybrid/exposed-collagen layer thickness. It is observed that the stress concentration factor at the adhesive/peritubular dentin interface decreases with the hybrid/exposed-collagen layer thickness. The stress concentration factor in the peritubular dentin shows marginal variation with the hybrid/exposed-collagen layer thickness.

Figure 7(a, b) gives the distributions of the Von Mises stress and the major principal stress in the unit cell with 4-and 10-μm hybrid/exposed-collagen layer, respectively. From the stress distributions in Figure 7, it can be seen that a thicker hybrid/exposed-collagen layer results in a visibly larger stress concentration Zone 1, even though the maximum stresses are about the same as the case with thinner hybrid/exposed-collagen layer. The larger stress concentration Zone 1 indicates an increased likelihood of failure initiating in this peritubular region for the cases with thicker hybrid/exposed-collagen layer caused by poor adhesive penetration or adhesive phase separations.

The effect of hybrid/exposed-collagen layer thickness upon stress distribution is illustrated by quantifying the nominal area of the stress concentration Zone 1 in the peritubular dentin. The nominal area is obtained by considering the region within the peritubular dentin, which has stresses larger than 60 MPa. Table III tabulates the stress range and the corresponding concentration zone area. It is noted that although the stress range in the concentration zone is similar for all the cases, the concentration-zone area increases with the hybrid/exposed-collagen layer thickness.

In Figure 8, the nominal area of the peritubular stress concentration zone is plotted against the hybrid/exposed-collagen layer thickness. Interestingly, the area of the peritubular stress concentration zone becomes increasingly bigger with the hybrid/exposed-collagen layer thickness. This stress distribution behavior indicates that the depth of dentin demineralization during etching clearly exacerbates the stress concentration problem within the peritubular dentin, and further suggests that the likely d/a interface failure initiation point lies within the peritubular dentin.

Effect of Peritubular and Intertubular Dentin Width on Stress Distribution

Because the density of tubules gradually decreases away from the internal pulp chamber, it is expected that the peritubular and intertubular dentin widths vary with distance from the pulp chamber. The effect of peritubular and intertubular dentin widths upon stress concentration in Zone 1 is illustrated in Figure 9, which gives a plot of the stress concentration factor, defined as the ratio of maximum major principal stress and the applied stress, and the intertubular dentin width. In these calculations, the thickness of the hybrid/exposed-collagen layer is taken to be 2 μm, and a linear profile is assumed for adhesive infiltration, such that the elastic moduli of the hybrid/exposed-collagen layer is graded from

4 to 1 GPa. All other micromechanical and microstructural parameters are kept the same. As seen from Figure 9, the stress concentration increases with the intertubular dentin width, whereas the other factors, such as the hybrid-layer thickness, are held constant. Furthermore, the stress concentration is found to be increasingly higher for thinner peritubular dentin width. Thus, the locations within the d/a interface that have the thinnest peritubular dentin and the widest intertubular dentin are the most vulnerable and the likely failure initiation points.

DISCUSSION

The premature failure of moderate to large composite restorations can be traced to a breakdown of the bond at the tooth surface/composite material interface[3,23,24] and increased levels of the cariogenic bacteria, *Streptococcus mutans*, at the perimeter of these materials.[25,26] The breakdown of this bond has been linked to the failure of current materials to consistently seal and adhere to the dentin.[27] Acid etching provides effective mechanical bonding between the composite restoration and treated enamel, but breakdown at the dentin surface continues to threaten the long-term viability of large posterior composite restorations.[24,25,28]

Current theories on dentin bonding suggest that two fundamental processes are involved in bonding an adhesive to dentin. First, the mineral phase must be extracted from the dentin substrate without altering the collagen matrix, and second, the voids left by the mineral must be filled with adhesive resin that undergoes complete *in situ* polymerization; that is; the formation of a resin-reinforced or hybrid layer. The ideal hybrid layer would be characterized as a three-dimensional collagen–resin biopolymer that provides both a continuous and stable link between the bulk adhesive and dentin substrate.

The hybrid layer has been described as the weakest link or Achilles heel of the d/a bond.[29] This characterization is based on the results of several *in vitro* investigations and a recent *in vivo* study, which point to breakdown of the hybrid layer in wet environments.[29–31] These results suggest that the hybrid layer does not form an impervious three-dimensional collagen/polymer network throughout the breadth of the demineralized dentin. Instead, the adhesive may undergo a physical oil-and-water separation as it interacts with the wet demineralized dentin.[16] The critical dimethacrylate component (BisGMA), which contributes the most to the cross-linked polymeric adhesive, infiltrates a fraction of the total demineralized, intertubular dentin layer.[12,16,32] A poor-quality hybrid layer can leave unreinforced and exposed collagen at the composite margin and/or beneath the restoration.

Understanding the role of the interface in dentin/adhesive bond failure requires *in situ* structure and property characterization, but there are limited techniques that provide this capability at the resolution of the hybrid layer. Two techniques that meet these requirements are: micro-Raman spectroscopy and scanning acoustic microscopy. Micro-Raman spectroscopy provided d/a interfacial structural analysis *in situ* at ≈1-μm spatial resolution.[11,12,16,32] The scanning acoustic microscopy provided *in situ* micromechanical property analysis of the d/a interface at ≈2.5-μm resolution.[13,14,33] The empirical data from these microstructure/property analyses were used in a two-dimensional elastic FE modeling to predict stress concentration and distribution at the d/a interface under tensile loading.

The finite element results indicate that the stresses concentrate in the peritubular dentin in proximity to the hybrid/exposed-collagen layer. As the thickness of the hybrid/exposed-collagen layer increases, the area of stress concentration zones increases. The stress concentrations in peritubular dentin are exacerbated for cases with lower elastic moduli or nonlinear gradation of elastic moduli in the hybrid/exposed-collagen layers. Based on the

results of the μRS and SAM investigations, the exposed-collagen layer is a result of incomplete adhesive infiltration and/or adhesive phase separation.[11–14,16,32,34] The larger stress concentration zones for interfaces with a thicker hybrid/exposed-collagen layer indicates an increased likelihood of failure initiating in the peritubular region close to the hybrid layer. The stress concentration is found to be higher for wider intertubular dentin and narrower peritubular dentin, illustrating the effect that modulus of elasticity and microstructure has upon stress distribution and concentration at the d/a interface.

The conventional opinion that the low elastic modulus as a result of phase separation in the adhesive could offer a mechanical advantage to the system is not true. In other words, based on previous investigations, a commercial adhesive with a relatively high concentration of hydrophobic components undergoes phase separation in the presence of water with the demineralized dentin matrix.[16] In a bonded joint such as occurs under ideal conditions at the d/a interface, the globules of resin (as a result of adhesive phase separation) distributed within the demineralized dentin matrix would potentially reflect defects within the joint that would inhibit an even transfer of stresses across the d/a interface. Although this may be true, one might expect that the stresses would dissipate quickly in the low modulus region. The results from the finite element analyses indicate this is not true, because the low modulus regions lead to stress concentration in relatively high elastic modulus regions.

In conclusion, even though the applied stress is considerably smaller than dentin strength, the stress concentration caused by interface geometry and interface-component elastic moduli will likely lead to an overall d/a interface strength that is considerably less than the individual strengths of the interface components. For the simple mode and loading case considered in the preliminary calculations, complex multiaxial stresses exist at the microscopic level; consequently, a mixed-mode fracture mechanism is more likely. Devising a full-depth-high modulus hybrid layer may considerably reduce the stress concentration zone and the magnitude of stress concentration in the peritubular dentin next to the hybrid/exposed-collagen layer. Further investigations are ongoing to better define the microstructural and mechanical properties of the d/a interface, refine the model assumptions, and develop a 3D viscoelastic FE model.

Acknowledgments

Contract grant sponsor: USPHS; contract grant number: DE12487

Contract grant sponsor: National Institute of Dental and Craniofacial Research

Contract grant sponsor: USPHS Major Instrumentation

Contract grant sponsor: National Institutes of Health; contract grant number: RR16710

References

1. Kidd EAM, Toffenetti F, Mjor IA. Secondary caries. Int Dent J. 1992; 42:127–138. [PubMed: 1500208]
2. Kidd EAM, Beighton D. Prediction of secondary caries around tooth-colored restorations: A clinical and microbiological study. J Dent Res. 1996; 75:1942–1946. [PubMed: 9033448]
3. Collins CJ, Bryant RW, Hodge KLV. A clinical evaluation of posterior composite resin restorations: 8-year findings. J Dent. 1998; 26:311–317. [PubMed: 9611936]
4. Hunter AR, Treasue ET, Hunter AJ. Increases in cavity volume associated with the removal of class 2 amalgam and composite restorations. Op Dent. 1995:2–6.
5. Van Meerbeek B, Vargas M, Satoshie I, Yoshida Y, Perdigao J, Lambrechts P, Vanherle G. Microscopy investigations. Techniques, results, limitations. Am J Dent. 2000 Nov; 13(Special Issue):3–18.

6. Nakabayashi N, Saimi Y. Bonding to intact dentin. J Dent Res. 1996; 75:1706–1715. [PubMed: 8952625]
7. Nakabayashi, N.; Pashley, DH. Hybridization of dental hard tissues. Tokyo, Japan: Quintessence; 1998.
8. Tam LE, Pilliar RM. Fracture surface characterization of dentin-bonded interfacial fracture toughness specimens. J Dent Res. 1994; 73:607– 619. [PubMed: 8163731]
9. Inokoshi S, Nakaoki Y, Shono T, Pereira PNR, Yamada T, Tagami J. Collagen layer collapse and inhibited resin penetration by dentin etching. J Dent Res. 1996; 75:389. (Abstract No. 2976).
10. Gwinnett AJ. Quantitative contribution of resin infiltration/hybridization to dentin bonding. Am J Dent. 1993; 6:7–9. [PubMed: 8329167]
11. Spencer P, Wang Y, Walker MP, Wieliczka DM, Swafford JR. Interfacial chemistry of the dentin/adhesive bond. J Dent Res. 2000; 79:1458–1463. [PubMed: 11005728]
12. Wang Y, Spencer P. Quantifying adhesive penetration in adhesive/dentin interface using confocal Raman microspectroscopy. J Biomed Mater Res. 2002; 59:46–55. [PubMed: 11745536]
13. Katz JL, Bumrerraj S, Dreyfuss J, Wang Y, Spencer P. Micro-mechanics of the dentin/adhesive interface. J Biomed Mater Res Appl Biomater. 2001; 58:366–371.
14. Katz, JL.; Spencer, P.; Wang, Y.; Wagh, A.; Nomura, T.; Bumrerraj, S. Structural, chemical and mechanical characterization of the dentin/adhesive interface. In: Lewandrowski, K.; Wise, D.; Trantolo, D.; Gresser, J.; Yaszemski, M.; Altobelli, D., editors. Tissue engineering and biodegradable equivalents: Scientific and clinical applications. New York: Marcel Dekker; 2002. p. 775-793.
15. Katz, JL.; Bumrerraj, S.; Dreyfuss, J.; Spencer, P.; Wang, Y.; Swafford, JR. Micromechanics, morphology, and chemistry direct at the dentin/adhesive interface. Proceedings of the IADR Meeting; 2000.
16. Spencer P, Wang Y. Adhesive phase separation at the dentin interface under wet bonding conditions. J Biomed Mater Res. 2002; 62:447– 456. [PubMed: 12209931]
17. Katz, JL.; Bumrerraj, S.; Dreyfuss, J.; Spencer, P.; Wang, Y.; Swafford, JR. Micro-techniques for the study of the dentin/adhesive interface. Sixth World Biomaterials Congress; 2000; Kamuela, Hawaii.
18. Kinney JH, Balooch M, Marshall GW, Marshall SJ. A micro-mechanics model of the elastic properties of human dentine. Arch Oral Biol. 1999; 44:813– 822. [PubMed: 10530914]
19. Van Noort R, Norooze S, Howard I, Cardew G. A critique of bond strength measurements. J Dent. 1989; 17:61– 67. [PubMed: 2659632]
20. Van Noort R, Cardew G, Howard I, Norooze S. The effect of local interfacial geometry on the measurements of the tensile bond strength to dentin. J Dent Res. 1991; 70:889– 893. [PubMed: 1827133]
21. Phrukkanon S, Burrow MF, Tyas MJ. The effect of dentine location and tubule orientation on the bond strengths between resin and dentine. J Dent. 1999; 27:265–274. [PubMed: 10193103]
22. Sano H, Ciucchi B, Matthews WG, Pashley DH. Tensile properties of mineralized and demineralized human and bovine dentin. J Dent Res. 1994; 73:1205–1211. [PubMed: 8046110]
23. Mair LH. Ten-year clinical assessment of three posterior resin composites and two amalgams. Quintessence Int. 1998; 29:483–490. [PubMed: 9807127]
24. Nordbo H, Leirskar J, von der Fehr FR. Saucer-shaped cavity preparations for posterior approximal resin composite restorations: Observations up to 10 years. Quintessence Int. 1998; 29:5–11. [PubMed: 9611469]
25. Dunne SM, Gainsford ID, Wilson NHF. Current materials and techniques for direct restorations in posterior teeth. Part 1: silver amalgam. Int Dent J. 1997; 47:123–136. [PubMed: 9448798]
26. Svanberg M, Mjor IA, Orstavik D. *Mutans Streptococci* in plaque from margins of amalgam composite, and glass-ionomer restorations. J Dent Res. 1990; 69:861– 864. [PubMed: 2109000]
27. Meiers JC, Kresin J. Cavity disinfectants and dentin bonding. Oper Dent. 1996; 21:153–159. [PubMed: 8957905]
28. Roulet JF. Benefits and disadvantages of tooth-coloured alternatives to amalgam. J Dent. 1997; 25:459– 473. [PubMed: 9604577]

29. Sano H, Yoshikawa T, Pereira PNR, Kanemura N, Morigami M, Tagami J, Pashley DH. Long-term durability of dentin bonds made with a self-etching primer, *in vivo*. J Dent Res. 1999; 78:906–911. [PubMed: 10326735]

30. Hashimoto M, Ohno H, Kaga M, Endo K, Sano H, Oguchi H. *In vivo* degradation of resin– dentin bonds in humans over 1 to 3 years. J Dent Res. 2000; 79:1385–1391. [PubMed: 10890717]

31. Burrow MF, Satoh M, Tagami J. Dentin durability after three years using a dentin bonding agent with and without priming. Dent Mater. 1996; 12:302–307. [PubMed: 9170998]

32. Wang Y, Spencer P. Hybridization efficiency of the adhesive dentin interface with wet bonding. J Dent Res. 2003; 82:141–145. [PubMed: 12562889]

33. Katz, JL.; Nomura, T.; Wagh, A.; Spencer, P.; Wang, Y. Micro-chemical and mechanical properties/structure relationships at the dentitional tissues–adhesive– composites interfaces. Structural Biomaterials for the 21st Century; Proceedings of the 2001 TMS Annual Meeting; 2001; New Orleans, LA.

34. Kadler KE, Holmes DF, Trotter JA, Chapman JA. Review article: Collagen fibril formation. Biochem J. 1996; 316:1–11. [PubMed: 8645190]

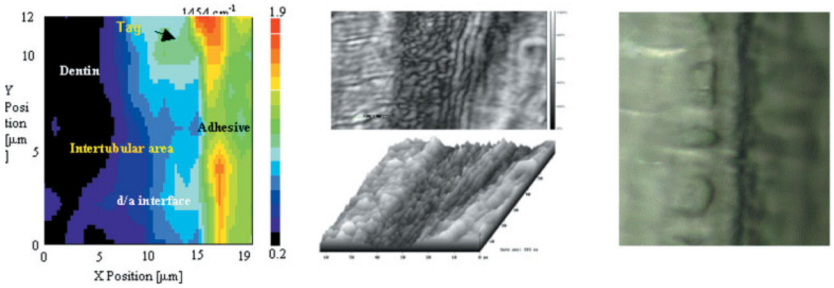

Figure 1.
Images obtained from μRS, SAM and optical microscope of the same small region different magnifications. [Color figure can be viewed in the online issue, which is available at www.interscience.wiley.com.]

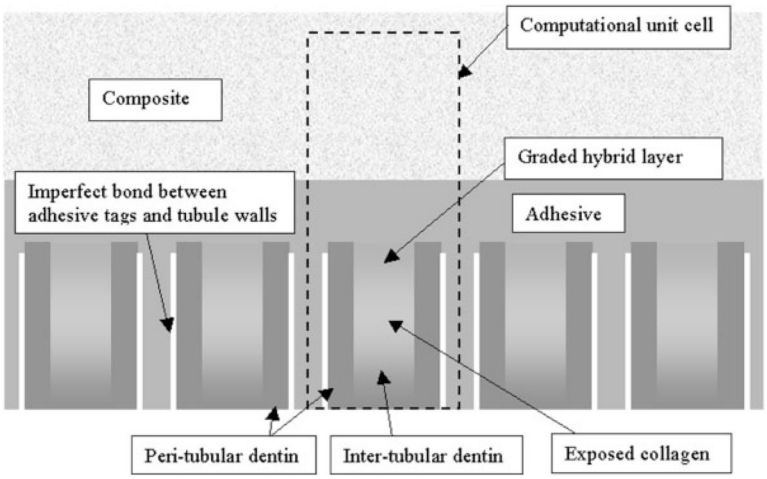

Figure 2.
Schematic view of dentin-adhesive interface.

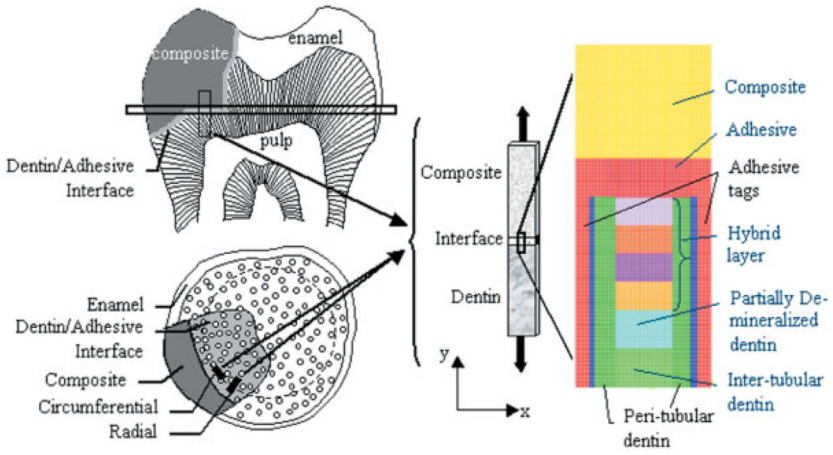

Figure 3.

Thin rectangular sample of restored tooth subjected to tensile loading, and the FEM mesh of a unit-cell of dentin-adhesive interface subjected to a tension load of 20 MPa. [Color figure can be viewed in the online issue, which is available at www.interscience.wiley.com.]

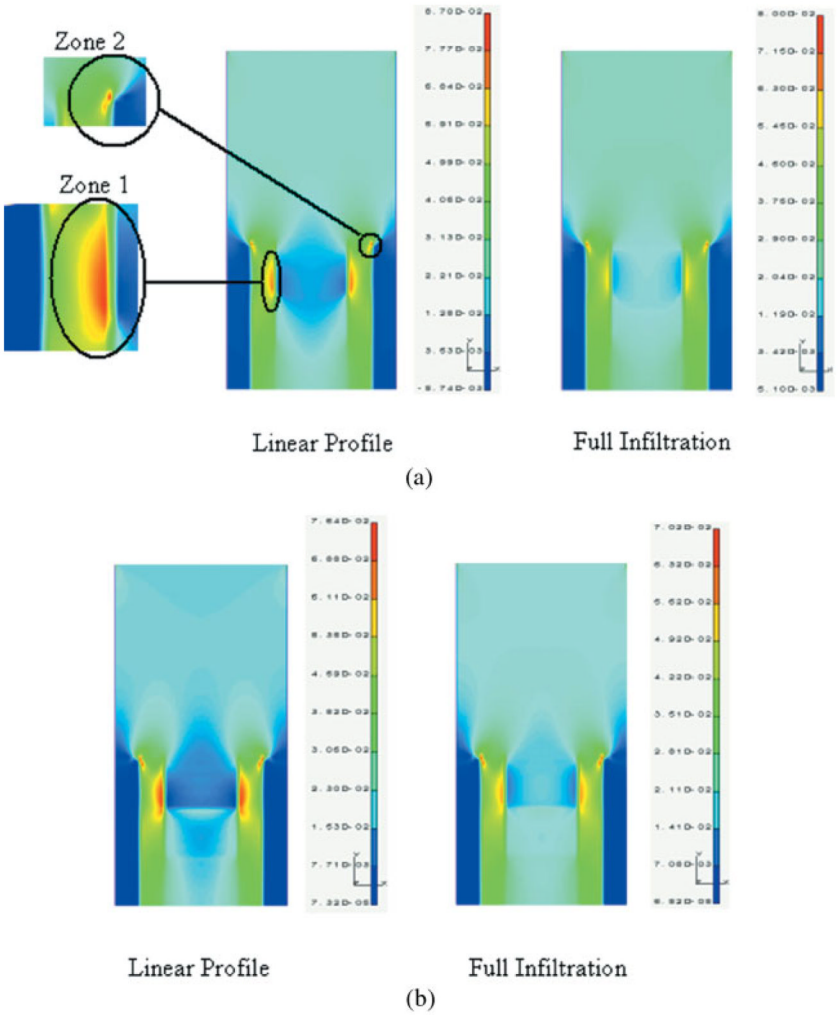

Figure 4.

(a) Major principal stress distribution in a unit cell of dentin/adhesive interface subjected to a tension of 20 MPa (stress units on the scale bar are in 10^3 MPa). (b) Von Mises stress distribution in a unit cell of dentin/adhesive interface subjected to a tension of 20 MPa (stress units on the scale bar are in 10^3 MPa). [Color figure can be viewed in the online issue, which is available at www.interscience.wiley.com.]

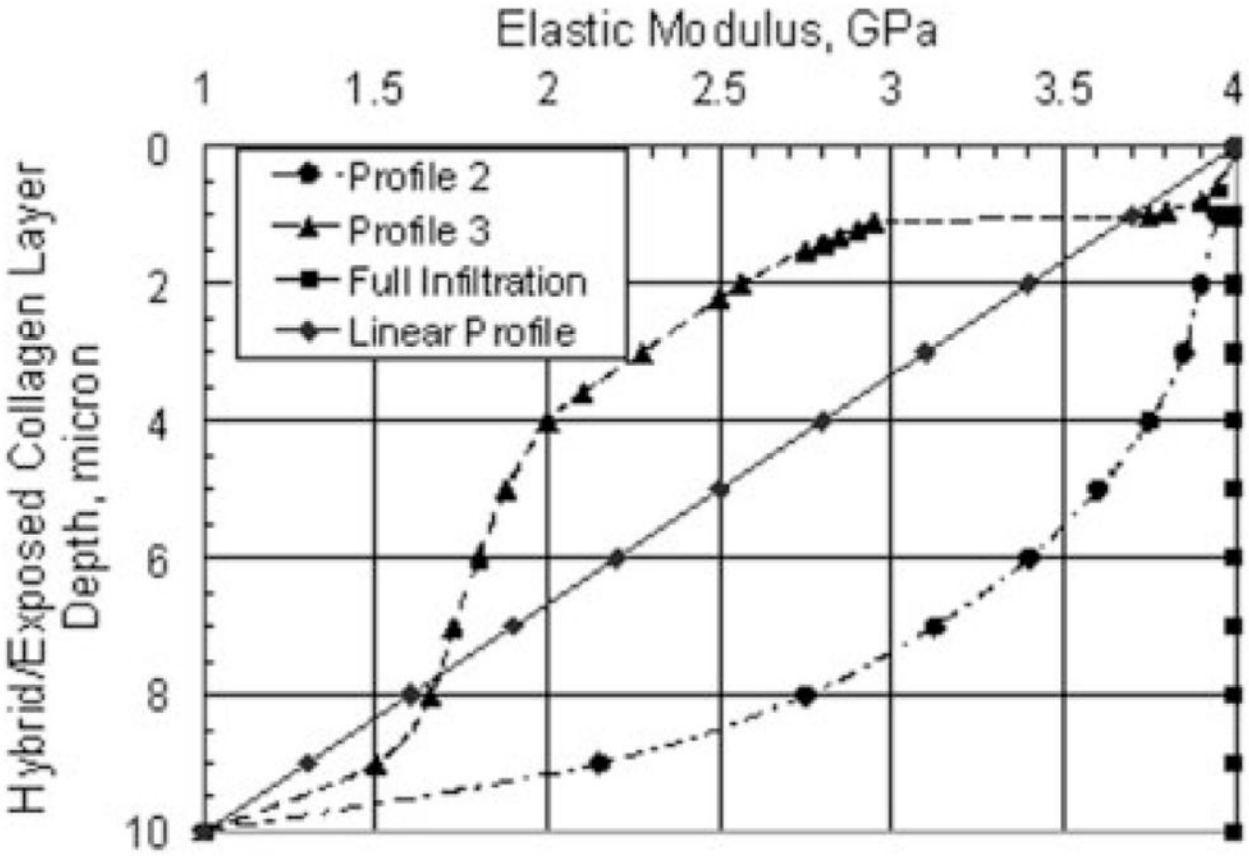

Figure 5.
Hybrid/exposed-collagen layer elastic moduli for different adhesive infiltration profiles.

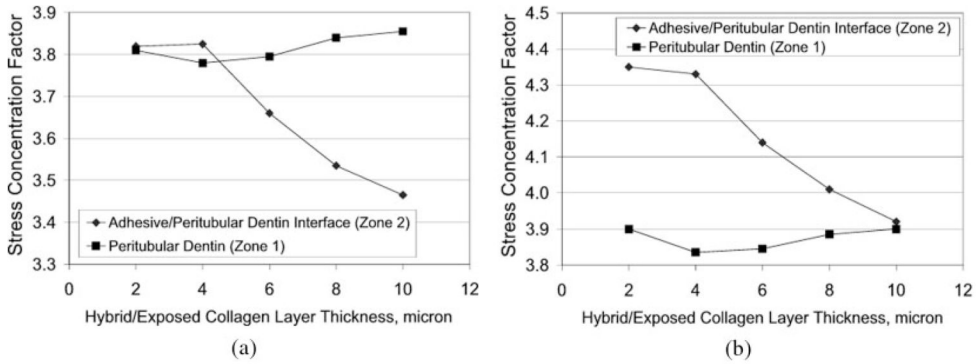

Figure 6.

Stress concentration factor variation with hybrid/exposed– collagen layer thickness: (a) Von Mises stress, and (b) major principal stress.

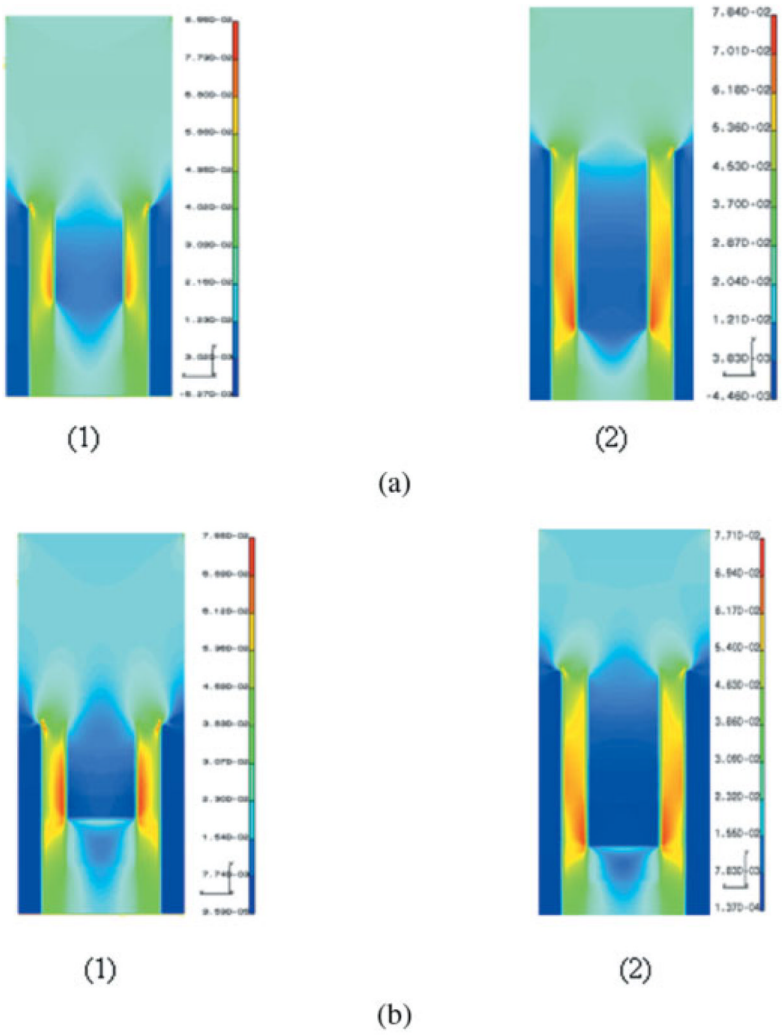

Figure 7.

(a) Major principal stress distribution in a unit cell of dentin adhesive interface with (1) 4-μm hybrid layer, and (2) 10-μm hybrid layer (stress units on the scale bar are in 10^3 MPa). (b) Von Mises in a unit cell of dentin/adhesive interface with (1) 4-μm hybrid layer, and (2) 10-μm hybrid layer (stress units on the scale bar are in 10^3 MPa). [Color figure can be viewed in the online issue, which is available at www.interscience.wiley.com.]

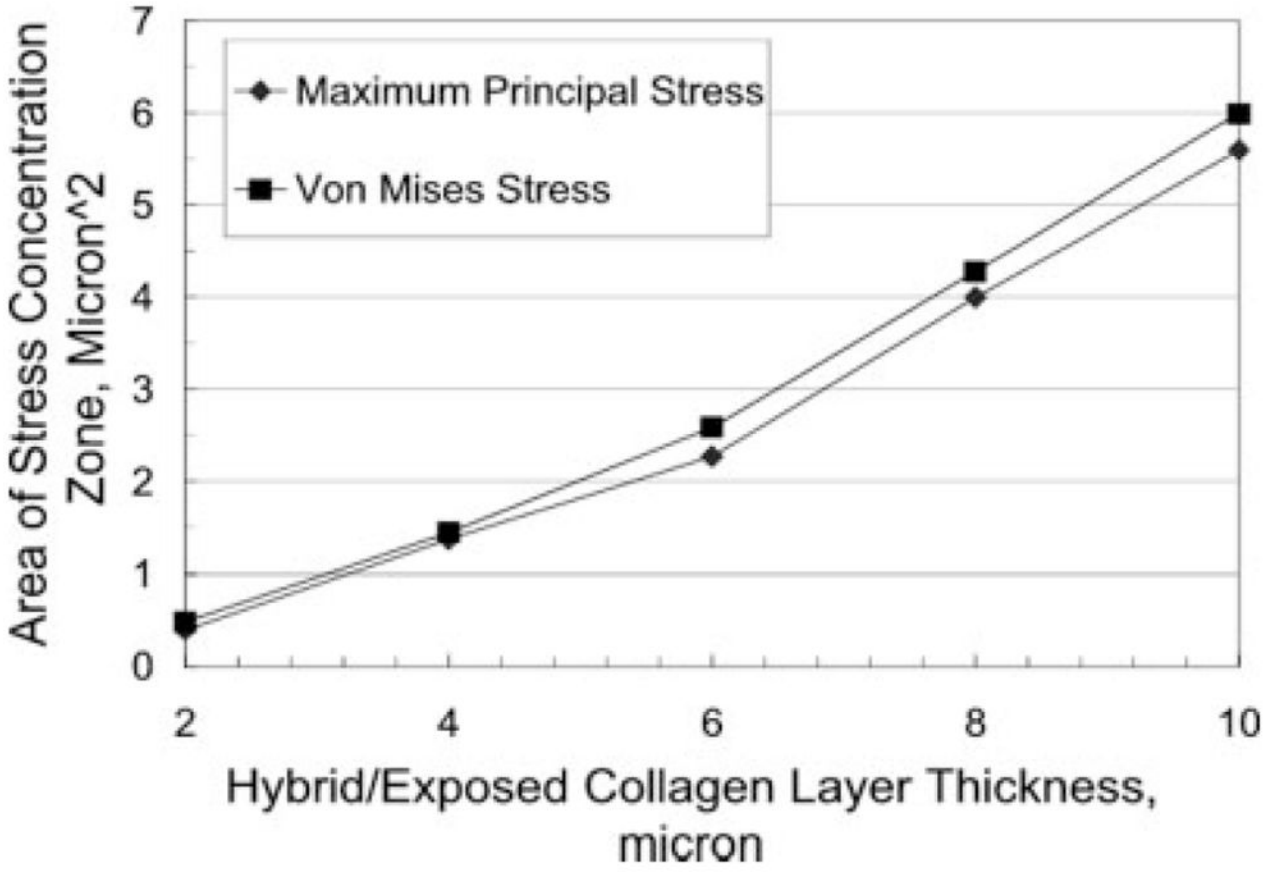

Figure 8.
Stress concentration Zone 1 nominal area variation with hybrid/exposed-collagen layer thickness.

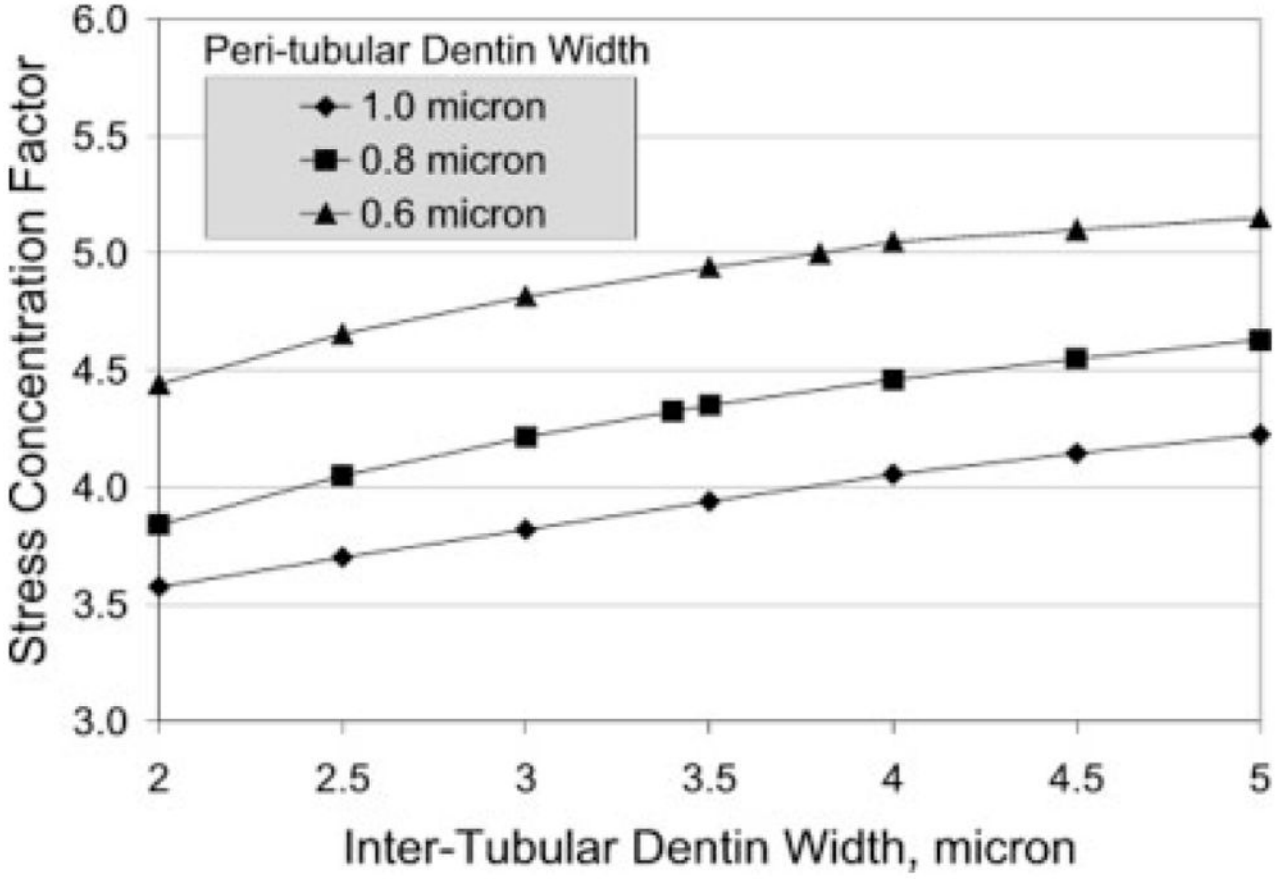

Figure 9.
Stress concentration factor variation with intertubular and peritubular dentin width.

TABLE I

Elastic and Geometrical Properties of Dentin/Adhesive Interface Components

Interface Component	Elastic Modulus (GPa)	Thickness (μm)
Composite	~30	
Adhesive	~5	2–5
Peritubular dentin[a]	26–30	0.6–1
Intertubular dentin[b]	13–20	2–5
Graded hybrid layer/exposed collagen[c]	5–1	2–10

[a] Based upon measurements by Kinney et al.[18]

[b] Based upon measurements by Kinney et al.[18] and Katz et al.[13] The intertubular dentin modulus was measured to be 20 GPa by Kinney et al.[18] Subsequently, Katz et al.[13] found that the intertubular dentin close to the interface has a lower modulus of 13 GPa due to partial demineralization during etching. Therefore in the vicinity of the interface, the intertubular dentin is considered to have a modulus gradient from 13 GPa ramping up to 20 GPa.

[c] Based upon measurements by Katz et al.[13]

TABLE II

Effect of Adhesive Infiltration Profiles on Stress Concentration at the d/a Interface Subjected to a Tension of 20 MPa

Adhesive Infiltration Profile	Von Mises Stress (MPa)	Major Principal Stress (MPa)
Full Infiltration		
Peritubular Dentin (Zone 1)	60.3	60.7
Adhesive/Peritubular Dentin Interface (Zone 2)	69.1	78.4
Profile 2		
Peritubular Dentin (Zone 1)	72.1	73.2
Adhesive/Peritubular Dentin Interface (Zone 2)	69.1	78.4
Linear Profile		
Peritubular Dentin (Zone 1)	75.6	76.7
Adhesive/Peritubular Dentin Interface (Zone 2)	70.1	79.4
Profile 3		
Peritubular Dentin (Zone 1)	75.0	76.0
Adhesive/Peritubular Dentin Interface (Zone 2)	72.1	81.6

TABLE III

Effect of Hybrid/Exposed Collagen Layer Thickness on Stress Concentration at the d/a Interface Subjected to a Tension of 20 MPa

	Von Mises Stress		Maximum Principal Stress	
Hybrid Layer Thickness (μm)	Concentration Zone Area (μm^2)	Stress Range (MPa)	Concentration Zone Area (μm^2)	Stress Range (MPa)
2	0.48	76.4–61.2	0.39	78.0–62.4
4	1.45	75.6–60.5	1.38	76.7–61.4
6	2.59	75.9–60.8	2.28	76.9–61.6
8	4.28	76.8–61.4	4.00	77.7–62.2
10	6.00	77.1–61.7	5.60	78.0–62.5